JOURNAL OF GEOPHYSICAL RESEARCH, VOL. 100, NO. B5, PAGES 8327–8338, MAY 10, 1995

Discrimination of fault planes from auxiliary planes based on simultaneous determination of stress tensor and a large number of fault plane solutions

Shigeki Horiuchi, Guillermo Rocco, and Akira Hasegawa
Observation Center for Prediction of Earthquakes and Volcanic Eruptions, Faculty of Science
Tohoku University, Sendai, Japan

Abstract. It is well known that there is a large difference in focal mechanism solutions of events even if they occur within a certain small area. Considering earthquake-generating stress to be uniform in a studied area, we developed a new method for simultaneously determining the stress tensor and the orientation of fault planes for many events by the use of polarity data of *P* waves. First, the number of inconsistent stations is calculated for various values of three parameters in the focal mechanism solution, with intervals of 10°. This calculation is made for all the events used. Then, four parameters defining the stress tensor are determined by a grid search using the data calculated above with the assumption that the slip direction in the fault plane should be parallel to the direction where the shear stress on the plane becomes maximum. A numerical test is made by applying the present method to an artificial data set composed of 25 events with 25 x 25 readings. It is found that a stable solution of the stress tensor is determined by the inversion and about 60% of fault planes are distinguished from auxiliary planes. There are no events whose auxiliary planes are incorrectly determined as fault planes. This method is used to estimate the earthquake-generating stress in the aftershock area of the 1984 western Nagano prefecture earthquake, central Japan. The results obtained show that the maximum principal stress is horizontal in the direction of N80°W-S80°E. There are strike-slip events having fault planes almost perpendicular to the fault plane of the main shock.

Introduction

Focal mechanism solutions of many earthquakes have been studied for a long time by many authors [e.g., *Honda et al.*, 1956; *Stauder*, 1964;*Wickens and Hodgson*, 1967; *Isacks and Molnar*, 1971]. Recently focal mechanism solutions for small events have been determined by using a large number of polarity data of initial motions of *P* waves obtained by dense seismic networks [e.g., *Ishida*, 1992;*Yamazaki et al.*, 1992; *Castillo and Ellsworth*, 1993]. These results show that many events with different orientations of focal mechanism solutions occur even in a small area with dimensions of a few kilometers.

Most of the events occurring in the San Andreas fault zone are strike-slip and one of the nodal planes is almost parallel to the San Andreas fault [*Jones*, 1988]. On the contrary, measurements of orientations of in situ stress made in the area near the San Andreas fault show that the direction of the maximum principal stress is almost perpendicular to the strike of the San Andreas fault [*Mount and Suppe*, 1987; *Zoback et al.*, 1987; *Shamir et al.*, 1988; *Zoback and Healy*, 1992]. There is a large difference in the orientation of the principal stress estimated from focal mechanisms of individual events and that by the in situ stress measurements.

Gephart and Forsyth [1984] considered that earthquakes occur along weak planes whose orientations are distributed randomly, and they developed a novel method to determine the stress tensor by assuming (1) the earthquake generating stress is uniform in a study area and (2) the slip direction of the fault is parallel to a direction where the shear stress becomes maximum. They developed a method to determine four parameters of the stress tensor by the use of a large number of focal mechanism solutions of events distributed in the study area. Their method is very effective in determining the state of stress, and it was applied to estimate the stress fields in Kaoiki, Hawaii [*Wyss et al.*, 1992], in the area near Baikal rift [*Doser*, 1991], and in the sinking Pacific plate [*Magee and Zoback*, 1993].

The second assumption above seems to be appropriate so long as fault motion is generated along a flat plane. There are two nodal planes in a focal mechanism solution. If a precise stress model is known, slip directions corresponding to both of the nodal planes can be predicted. Therefore it is possible to compare them to observed slip directions of the focal mechanism solution. In the case where there is a large discrepancy between the predicted and observed slip directions for one of the nodal planes, the plane with the large discrepancy is not likely to be the fault plane. *Urbancic et al* [1993] estimated orientations of fault planes by applying Gephart and Forsyth method to focal mechanism solutions of microseismic events which were determined by using polarity data observed at 64 and 32 stations at two mines.

However, in general, there is a large estimation error in individual focal mechanism solutions, especially in solutions determined by the use of a small number of *P* wave polarity observations. The large amount of estimation error makes it difficult to distinguish the fault plane from the auxiliary plane. Actually, most of the authors who use Gephart and Forsyth's method do not determine orientations of the fault planes. It is

Paper number 94JB03284.
0148-0227/95/94JB-03284$05.00

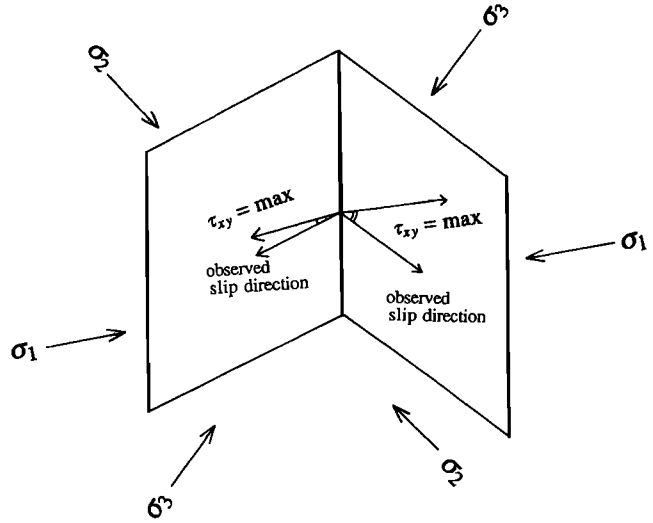

Figure 1. Schematic illustration showing observed slip directions and directions of the maximum shear stress in the two sheets of the nodal planes. Since the two directions of the maximum shear stress are not always perpendicular to each other, there is a difference in δ_1 and δ_2, which are angles between the slip direction in the focal mechanism solution and the direction of maximum shear stress for the fault plane and between the slip direction and that for the auxiliary plane.

not easy to determine a precise estimation error of each solution from the calculated parameters of focal mechanism solutions. This makes it difficult to estimate whether discrepancies between calculated and observed slip directions are smaller than or larger than observation errors. Therefore it is rather difficult to say that the fault plane is definitely distinguished from the auxiliary plane. However, if original data of P wave polarity readings are used, it is possible to estimate whether these discrepancies are smaller or larger than the observation error.

In the present study, considering the existence of a large estimation error in the individual focal mechanism solutions, we developed a new method to determine simultaneously the stress tensor and the orientations of fault planes. This method was applied to determination of the stress tensor in the western part of Nagano Prefecture, central Japan where a destructive earthquake of M6.8 occurred in 1984.

Theory

The stress field is assumed to be uniform in a study area, and earthquake faults occur along weak planes which are distributed randomly. A double-couple focal mechanism solution has two sheets of nodal planes. If one of the nodal planes is assumed to be the fault plane, the slip direction of the faulting is determined from observed polarity data (Figure1). Similar to *Gephart and Forsyth* [1984], we also assume that the slip direction of the faulting is parallel to a direction where the shear stress becomes maximum. The goal of the present work is to determine simultaneously parameters of the stress tensor and the orientation of fault planes for many events by the use of P wave polarity data.

There are six (6) independent components in the stress tensor. We put values of the principal stress to be σ_1, σ_2, and σ_3, where $\sigma_1 > \sigma_2 > \sigma_3$. The hydrostatic term is neglected by putting

$$\sigma_1 + \sigma_2 + \sigma_3 = 0. \tag{1}$$

Since P wave polarity data are used, absolute values of stress tensor are not determined. The ratio among values of the principal stress is given as

$$R = (\sigma_1 - \sigma_2)/(\sigma_1 - \sigma_3) . \tag{2}$$

It should be noted that values of σ_1, σ_2, and σ_3 are expressed by the use of R and a constant defining absolute values.

Let us make X_g Y_g, and Z_g three unit vectors defining geographical coordinates and P, B, and T the maximum (σ_1) the intermediate (σ_2), and the minimum (σ_3) principal stresses, respectively. By letting θ_P and ϕ_P be the inclination and azimuth for the vector P, as shown in Figure 2, P is given as

$$P = X_g \cos\phi_P \sin\theta_P + Y_g \sin\phi_P \sin\theta_P + Z_g \cos\theta_P . \tag{3}$$

The two vectors B and T are expressed by a function of rotation angle ω_P about P,

$$B = B_0 \cos\omega_P + T_0 \sin\omega_P , \tag{4}$$

$$T = -B_0 \sin\omega_P + T_0 \cos\omega_P , \tag{5}$$

where B_0 and T_0 are

$$B_0 = PZ_g / |PZ_g|, \tag{6}$$

$$T_0 = PB_0 . \tag{7}$$

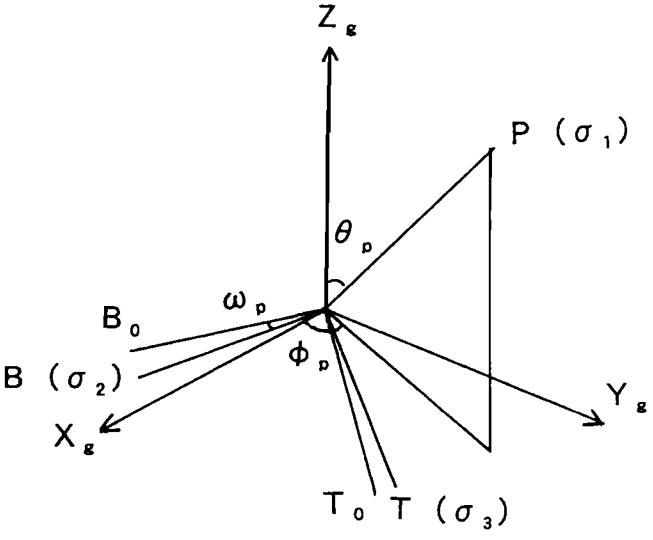

Figure 2. A Cartesian coordinate system showing the coordinates of geography (X_g, Y_g, Z_g) and that of the principal stresses (P, B, T). The vector B_0 is taken to a direction perpendicular to P and also Z_g. The directions of B and T are obtained by a rotation of B_0 and T_0 about P an amount of ω_P.

We assign X_i as a vector perpendicular to the fault plane for ith event. We call the direction of X_i the pole of the fault. By using angles of inclination θ_i and azimuth θ_i of the vector X_i measured in the (P, B, T) coordinate, X_i is given as

$$X_i = P\cos\phi_i \sin\theta_i + B\sin\phi_i \sin\theta_i + T\cos\theta_i . \quad (8)$$

A vector Y_0, which is perpendicular to T and also to X_i, is defined as

$$Y_0 = X_i T / |X_i T| . \quad (9)$$

By putting

$$Z_0 = X_i Y_0 , \quad (10)$$

the vectors Y_i and Z_i can be expressed by

$$Y_i = Y_0 \cos\omega_i + Z_0 \sin\omega_i \quad (11)$$

$$Z_i = -Y_0 \sin\omega_i + Z_0 \cos\omega_i \quad (12)$$

where ω_i is an angle between Y and Y_0. The direction of Y_i is perpendicular to the auxiliary plane.

Because $-X_i$ and $-Y_i$ are also perpendicular to the fault plane and to the auxiliary plane, respectively, it is necessary to make clear the signs of X_i and Y_i. We define vectors X_i and Y_i as

$$X_i = (P_m + T_m)/\sqrt{2} , \quad (13)$$

$$Y_i = (-P_m + T_m)/\sqrt{2} , \quad (14)$$

where P_m and T_m are unit vectors for the pressure and tension axes in the focal mechanism, respectively.

The shear stress in the fault plane is expressed as

$$\tau_{xy} = c_1 \cos\omega_i + c_2 \sin\omega_i = (c_1^2 + c_2^2)^{1/2} \sin(\omega_i + \omega_0) , \quad (15)$$

where c_1, c_2, and ω_0 are

$$c_1 = \cos\omega_i \cos\theta_i \sin\phi_i \cos\phi_i (\sigma_1 + \sigma_2) , \quad (16)$$

$$c_2 = \sin\omega_i \sin\theta_i \cos\theta_i \left(\sigma_1 \cos^2\phi_i - \sigma_2 \sin^2\phi_i - \sigma_3\right) , \quad (17)$$

$$\omega_0 = \tan^{-1}(c_1/c_2). \quad (18)$$

Gephart and Forsyth's assumption is that the slip direction should be parallel to a direction where shear stress becomes maximum. Equation (15) becomes maximum when $\omega_i + \omega_0 = \pi/2$, and becomes minimum when $\omega_i + \omega_0 = -\pi/2$. Since the signs for X_i and Y_i are taken in order that they satisfy equations (13) and (14), the shear stress becomes minimum in the slip direction. Therefore we have the equation

$$\omega_i = \omega_0 - \pi/2 , \quad (19)$$

Putting (19) into (11) yields the slip direction in the case that the pole of the fault is expressed in (8).

The theoretical amplitude of the P wave is given as

$$S_{ij} = C\,(A_{ij} X_i)(A_{ij} Y_i) \quad (20)$$

where C and A_{ij} are a constant and a unit vector showing the direction of jth station for ith event, respectively. The number of inconsistent stations is calculated by comparing polarity of theoretical amplitudes to that of observations. Equation (20) is a function of the four parameters of the stress tensor, R, θ_P, ϕ_P, and ω_P, and the two parameters for the pole of the fault plane. Therefore the total number of inconsistent stations is a function of these parameters and can be expressed in the form

$$N_{tot} = \sum_i \sum_j N_{ij}(\theta_P, \phi_P, \omega_P, R, \phi_t, \theta_t, A_{ij}, P_{ij}) , \quad (21)$$

where P_{ij} and N_{ij} are a reading of a P wave polarity and a value of the inconsistency, which becomes 0 when the polarity of the theoretical amplitude agrees with that of the observation and becomes 1 when it does not.

Since polarity data are used that are compressional or dilatational showing only the sense of initial motion of P waves, the best fit solution is determined under a criterion that the total number of stations having inconsistent observations becomes minimum. It is difficult to calculate derivatives of (21) because they become infinite on the nodal planes. Therefore the inversion is made numerically.

The total number of unknown parameters is $4 + 2N_{eq}$, where N_{eq} is the number of events used in the analysis. Clearly the number of inconsistent stations for an event is independent of directions of fault planes for other events. Therefore it is not necessary to make a grid search corresponding to all combinations of unknown parameters. The best fit solution is searched only by calculating (21) for all cases of the four parameters of the stress tensor with intervals of a certain value. The total number of the inconsistent stations can be written in the form

$$N_{tot} = \sum_i M_i(\theta_P, \phi_P, \omega_P, R), \quad (22)$$

where M_i is the minimum number of inconsistent stations for the ith event in a case when values of the four parameters of the stress tensor are θ_P, ϕ_P, ω_P, and R. It takes a great deal of computation time to make the grid search with intervals of a certain value because it is necessary to determine M_i for all cases of four parameters. Thus first numbers of inconsistent stations are calculated for all cases of ϕ_i, θ_i, and ω_i, which are three parameters defining the orientation of the focal mechanism solution for ith event, with intervals of a certain degree. This calculation is made for all events. All calculated values are stored. Then M_i in (22) is determined by the use of these data.

Since there are discontinuities in the seismic velocity structure within the Earth, there are many cases where takeoff angles for many stations are distributed in a very narrow angle range. Therefore it is very important to make a grid search as precise as possible. The calculation of numbers of inconsistent stations is made by the use of the program developed by *Horiuchi et al.* [1972]. This program has the advantage that the amount of the computation time of the grid search about three parameters is almost independent of one parameter ω_i which is a rotation angle around X_i. This is caused mainly by the fact

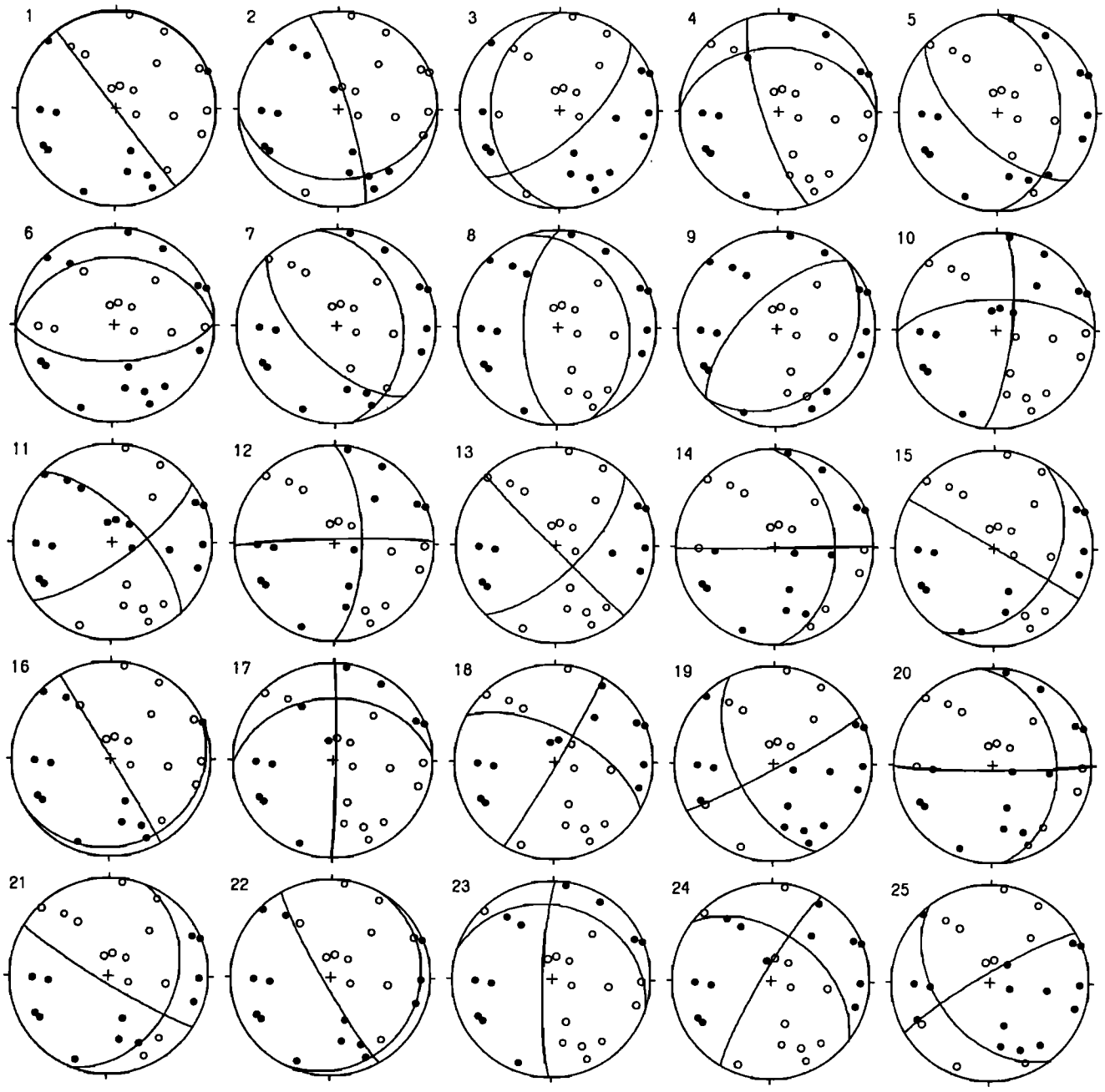

Figure 3. Equal area projections on the lower focal hemisphere showing the distribution of polarity data used in the numerical test.

that their method first calculates a value of rotation angles around X_i from each station to the initially assumed location of the nodal plane, which is defined by Y_0 and Z_0 in (9) and (10). These values are used to compute numbers of inconsistent stations at all values of ω_i within a certain interval. Actually, numbers of inconsistent stations are calculated with intervals of 0.2° for ω_i, and the minimum value in each interval range of 3° is stored.

The total number of data for numbers of inconsistent stations is $N_{eq} \times N_X \times N_W$, where N_x and N_W are numbers of grid points for the pole of the fault plane and those for the rotation angle around the pole, respectively. In the case of using 100 events, intervals of 5° for X_i and 3° for ω_i, the total capacity of data becomes $100 \times 685 \times 30 \times 2 = 4.11$ Mbyte, which can be stored on the memory of a work station having a moderate throughput during the calculation of the inversion.

Gephart and Forsyth [1984] noticed that it is necessary to choose one of the nodal planes to be the fault plane in the stress inversion of their method. This choice is based on values of differences between observed slip directions and theoretical slip directions. Since the present method makes a grid search by changing the pole of the fault plane to all directions, we do not need to take into account this choice.

Numerical Testing

A numerical test is made by applying our method to an artificial data set. We assume the stress field is uniform and

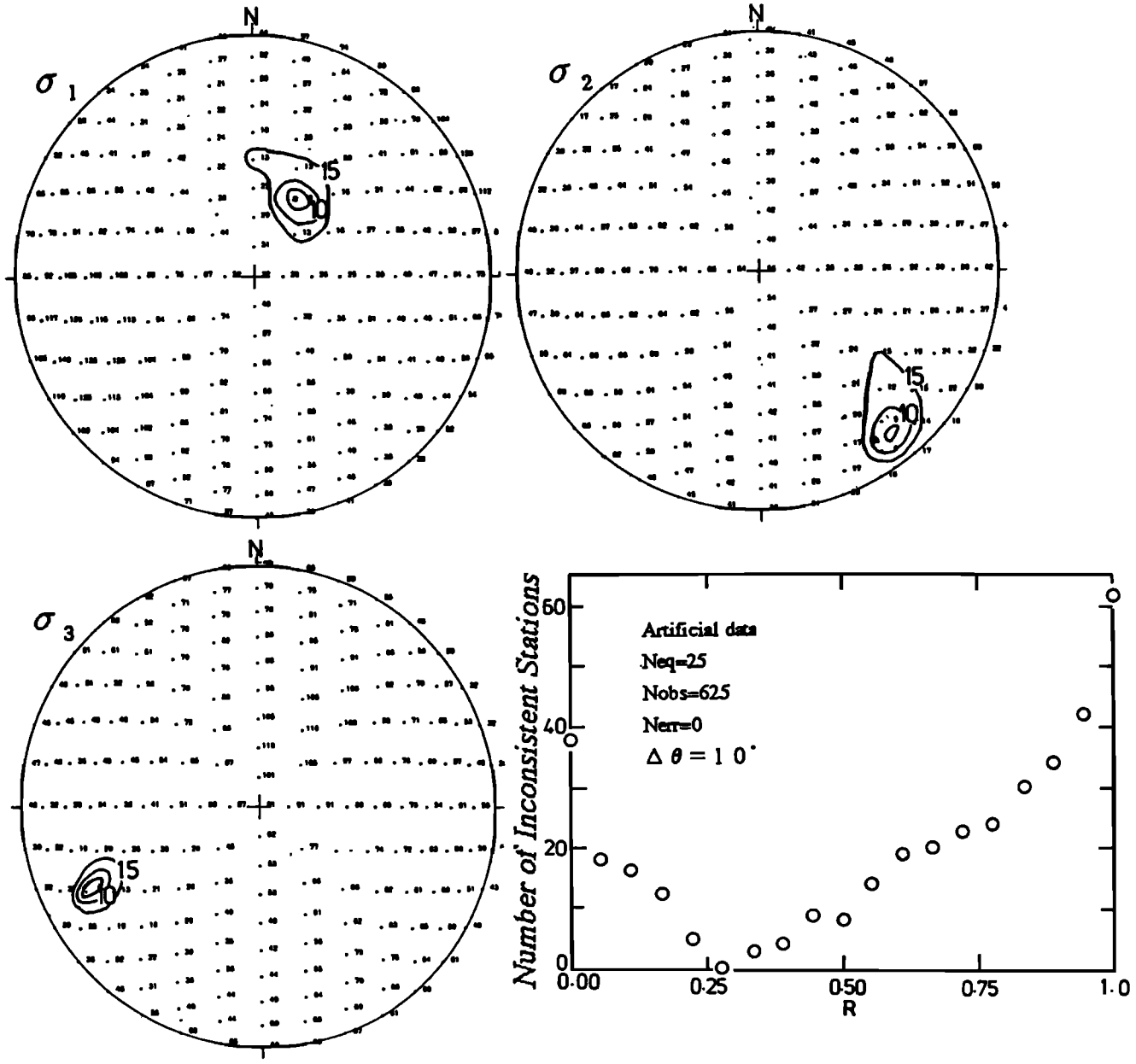

Figure 4. Equal-area projections showing permissible ranges of orientations of the principal stresses determined by the use of the artificial data set shown in Figure 3. Numerals near contour lines indicate the total number of inconsistent stations. The bottom right shows the distribution of the total numbers of inconsistent stations against variations of R.

generates earthquakes whose fault planes are oriented in random directions. The slip direction corresponding to each fault is assigned so that the shear stress defined in the fault plane becomes minimum in the direction of the dislocation. Artificial polarity data are obtained from values of the theoretical amplitude calculated from the geometry of the fault plane and that of the stations. The artificial data are composed of 25×25 polarity data from 25 events. Figure 3 shows distributions of stations projected on the focal spheres. The artificial data are generated by setting ω_P, θ_P, ϕ_P, and R to 30°, 30°, 30°, and 0.3°, respectively. Focal mechanism solutions for individual events are calculated from the artificial data, and they are also shown in Figure 3.

Although the amount of computation time is greatly decreased by using data for numbers of inconsistent stations, which are first calculated for all cases of only three parameters of the focal mechanism solutions and stored, it still takes 2 days to obtain the best fit solution in a case of a grid search with intervals of 5° using a work station with a moderate throughput. Therefore the following calculations are made with intervals of 10° except for the parameterω_i which is searched with intervals of 0.2°.

Since it is very important to calculate permissible ranges in the unknown parameters, we determined the distributions of numbers of inconsistent stations by putting directions of principal stresses to all directions with certain intervals and by making a grid search against the other unknown parameters. The distributions of the minimum number of inconsistent stations for the maximum, the intermediate, the minimum principal stresses and R are shown in Figure 4. The number of

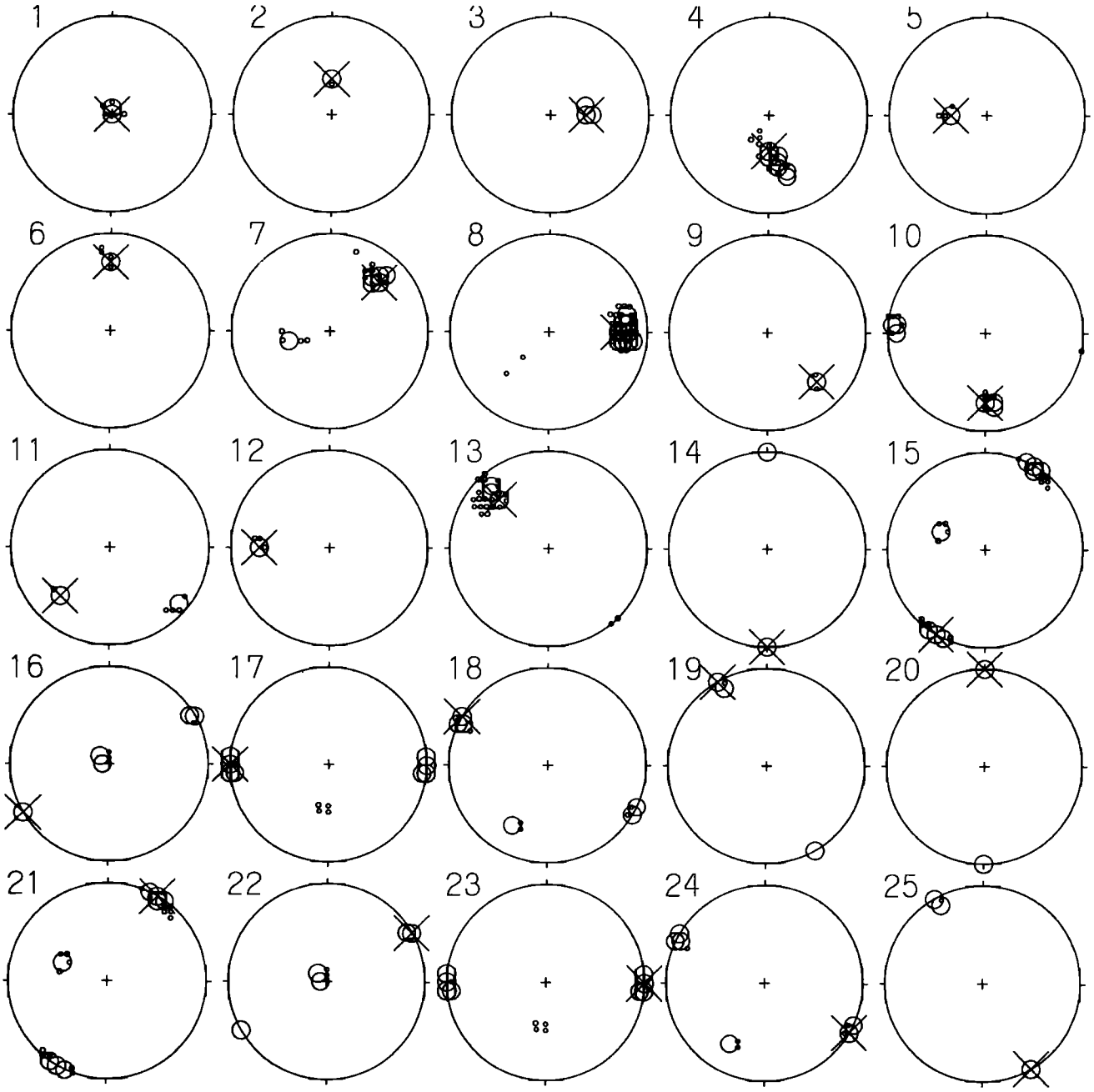

Figure 5. Equal-area projections showing the result of the numerical testing for discriminating fault planes from auxiliary planes. Crosses and circles indicate the directions perpendicular to fault planes given in the artificial model of numerical testing and those estimated in the inversion, respectively. Large and small circles indicate directions where numbers of inconsistent stations are 0 and 1, respectively.

inconsistent stations is 0 at the given stress model of the artificial data. The number of inconsistent stations is larger than 10 in all areas except for a small area near the original artificial model. Variations of the total number of inconsistent stations against R are also shown in Figure 4. The number of inconsistent stations is less than 10 in a range from 0.2 to 0.5 and less than 20 in a wide range from 0.05 to 0.6. This result suggests the difficulty of determining a precise value of R.

Permissible ranges of the location of the poles of fault planes are estimated by using the inverted model of the stress tensor. Figure 5 indicates equal area projections showing the location of the pole of the fault plane for each event. Large and small circles denote directions where the numbers of inconsistent stations are 0 and 1, respectively. Crosses indicate the locations of poles used to calculate artificial data. The number of inconsistent stations is 0 near the crosses. The result for 16 cases, i.e., except for events 7, 10, 11, 15, 16, 18, 21, 22, and 24, shows that directions without inconsistent stations are limited to a small area near the crosses. The other nine results have a minimum at directions nearly perpendicular to the crosses. Thus we can distinguish fault planes from auxiliary planes in 16 cases and cannot in nine cases. There are no events whose auxiliary plane is incorrectly determined as the fault plane.

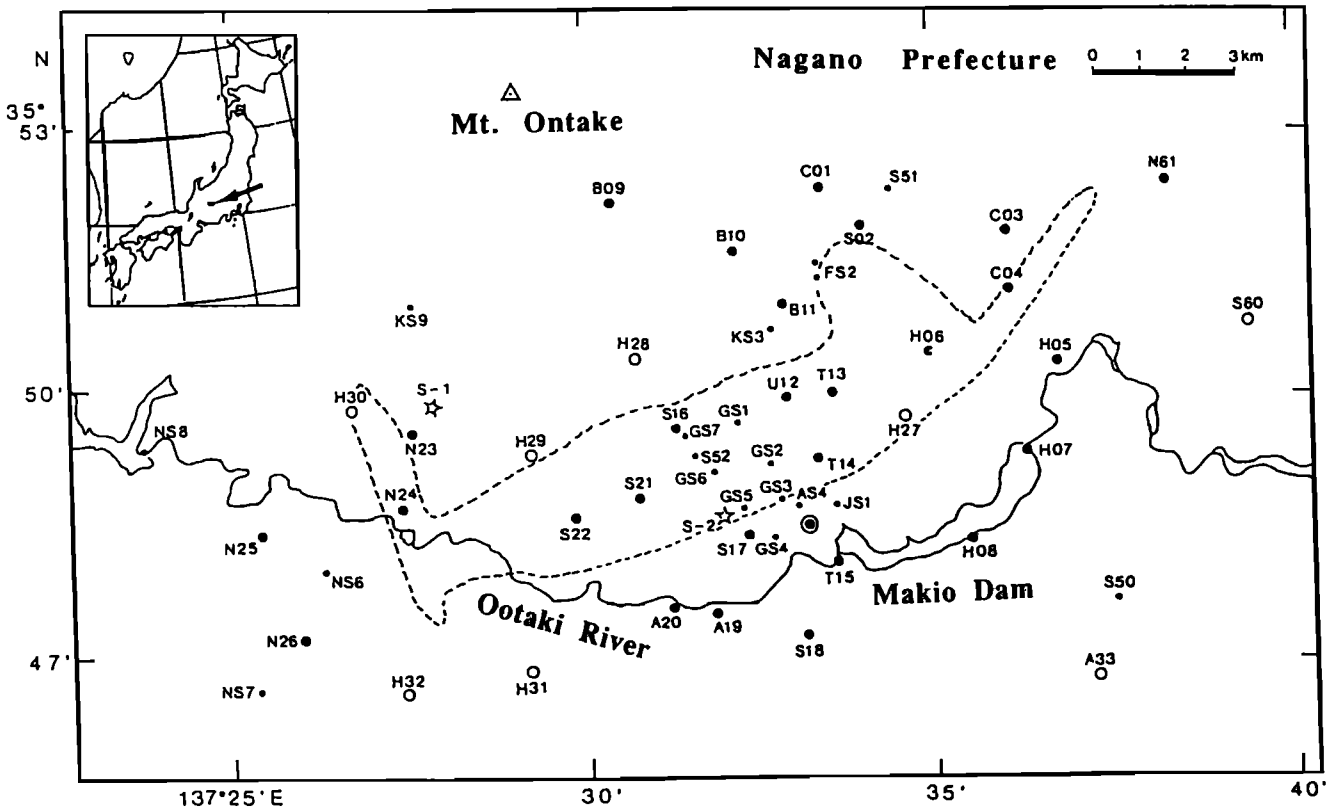

Figure 6. Map showing the locations of the observation stations set up by *Group for the Seismological Research in western Nagano prefecture* [1989]. Large solid circles indicate telemetered stations. The double circle indicates the observation center for the telemetered stations. The region enclosed by the dashed line indicates aftershock area obtained by the joint aftershock observation by Nagoya University and Tohoku University made just after the occurrence of the 1984 western Nagano prefecture earthquake [*Horiuchi et al.*, 1985]

Stress Field in the Western Part of Nagano Prefecture

A destructive earthquake, the 1984 western Nagano prefecture earthquake with $M6.8$ occurred in the central part of Japan on September 14, 1984. It was a right-lateral fault with a strike of N70°E and about 12 km length [*Ooida et al.*, 1989]. Many aftershocks were observed. The focal area of the main shock is located at the southern base of an active volcano called Mount Ontake, which erupted in 1976 [*Aoki et al.*, 1980]. An active earthquake swarm had been occurring around the focal area since 1976 [*Ooida et al.*, 1989].

As shown in Figure 6, a dense temporary seismic network was set up in the aftershock area in 1986 by the *Group for the Seismological Research in Western Nagano Prefecture* [1989]. They set 57 stations including 27 telemetry stations in a small area with about 20 km in the east-west and 12 km in the north-south direction. Seismograms for about 1500 events occurring inside and outside the network were obtained during 52 days of observations from September to October, 1986, about 2 years after the occurrence of the main shock. They employed a real-time automatic system using personal computer developed by *Horiuchi et al.* [1992a], which can detect, record, and locate seismic events. Preliminary hypocenters of about 1200 aftershocks were located by the real-time system. Precise hypocenters for 550 events inside and outside the network were located by using the data from the 57 stations shown in Figure 7 [*Horiuchi et al.*, 1992b]. A large spatial variation in the greatest depth of the aftershock area was found from the aftershock distribution. *Mizoue and Ishiketa* [1988] and *Inamori et al.* [1992] detected two sheets of midcrustal S wave reflectors beneath the focal region of the main shock, one of which is nearly parallel to the cutoff depth of aftershocks and the upward extension of the other coincides with the western end of the aftershock area.

Polarity data of P waves are also measured. Since a very dense seismic network was set up just above the aftershock area, observation stations projected on the focal sphere cover a wide area. Focal mechanism solutions for about 550 events determined by *Yamazaki et al.* [1992] show that there are four regions having different types of mechanisms. Their result also suggests that events of strike-slip and reverse faulting are distributed in a very narrow region in the aftershock area.

Relatively large events deeper than 4 km and enclosed by the large rectangle in Figure 7 are used in the stress tensor inversion developed in the present study. Only events having more than 20 readings of polarity data are used. Moreover, we do not use data for events having two or more inconsistent stations in individual focal mechanism solutions. There are 167 total events and 4980 total polarity data. The total number of inconsistent stations for all of the individual focal mechanism solutions is 77.

The result of the stress tensor inversion is shown in Figure 8. The orientation of the maximum stress is nearly horizontal and N80°W. Directions having a small number of inconsistent

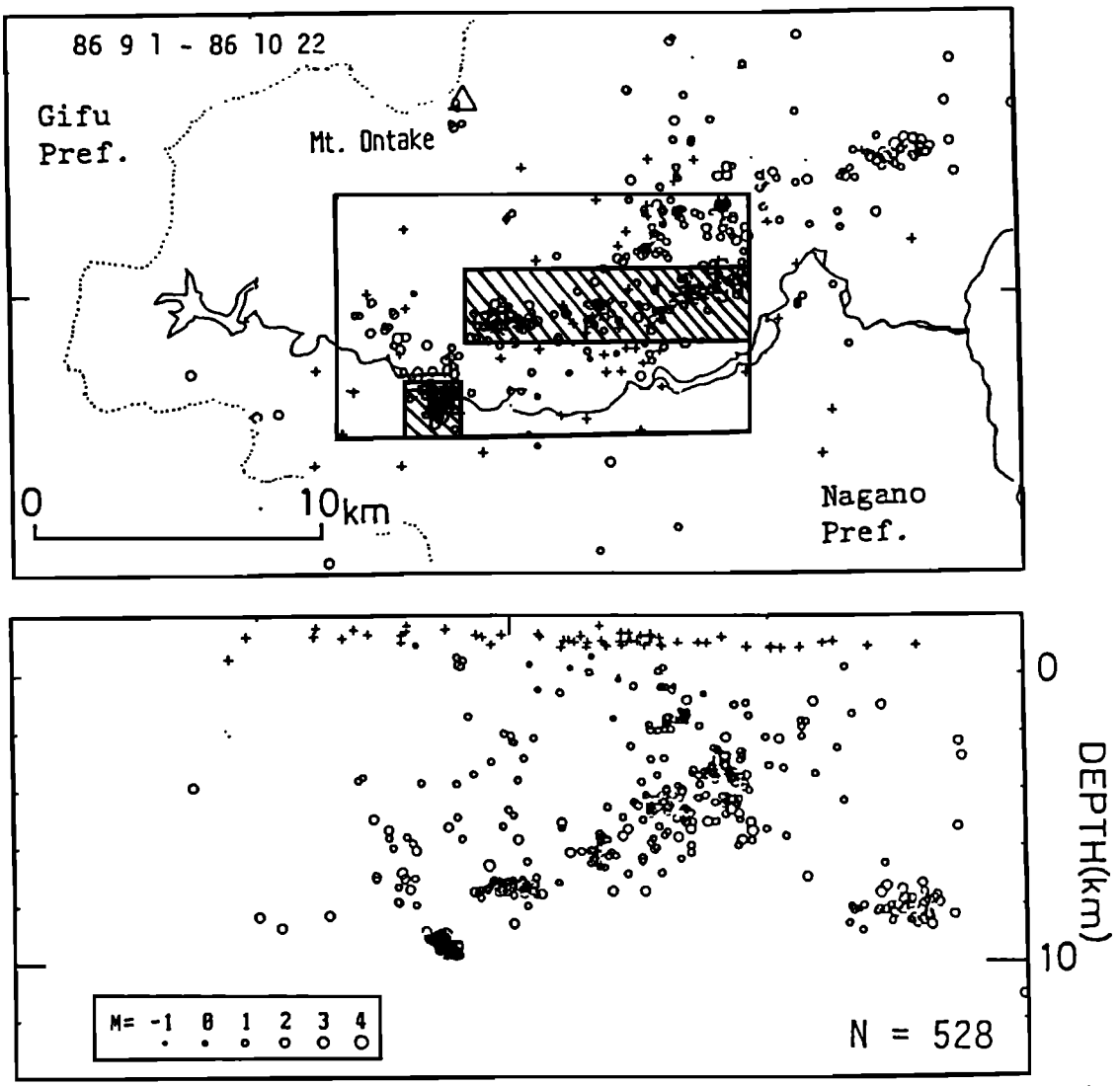

Figure 7. Map showing hypocenter distribution of aftershocks determined by *Horiuchi et al.* [1992b]. Pluses indicate observation stations. Polarity data for events that occurred in the large rectangle are used in the inversion.

stations are limited to a narrow region which is elongated in the horizontal plane. The orientation of the intermediate and the minimum principal stresses are in the north and south directions with plunge angles of 15° and 60°, respectively. The contours for these principal stresses shown in Figure 8 indicate that permissible areas for these directions are small. The obtained value of R is 0.6. The number of inconsistent stations in the best fit solution is 167 and is less than 180 for values of R ranging from 0.3 to 0.8.

We estimated permissible ranges of the orientation of fault planes for individual events by the use of the obtained parameters of the stress tensor. The estimation is made by calculating numbers of inconsistent stations for all values of strike and dip angles of the fault plane with certain intervals. Stereonet projections in Figures 9 and 10 show directions of fault planes for events occurring in the shaded regions of the central and south-western parts of the studied areas (Figure 8), respectively. Fault planes having the minimum number of inconsistent stations are plotted. We can see from Figures 9 and 10 that the orientations of fault planes for about 50% of events are determined uniquely. Since the result for the other 50% has two nodal planes which are nearly perpendicular to each other, the orientations of fault planes for these events cannot be distinguished from auxiliary planes.

The main shock of the 1984 western Nagano prefecture earthquake is a strike-slip fault with strike N80°E-S80°W. The inverted fault planes for about onethird of events are strike-slip faults similar to the main shock. There are strike-slip events with fault planes nearly perpendicular to that of the main shock.

Discussion

We developed a new inversion technique which simultaneously determines the stress tensor and the orientations of fault planes for many events by the use of polarity data. A numerical approach for the grid search is taken to determine solutions having the minimum number of inconsistent stations. *Gephart and Forsyth* [1984] developed a stress tensor inversion technique. The difference between the method by *Gephart and Forsyth* [1984] and the present method is that the

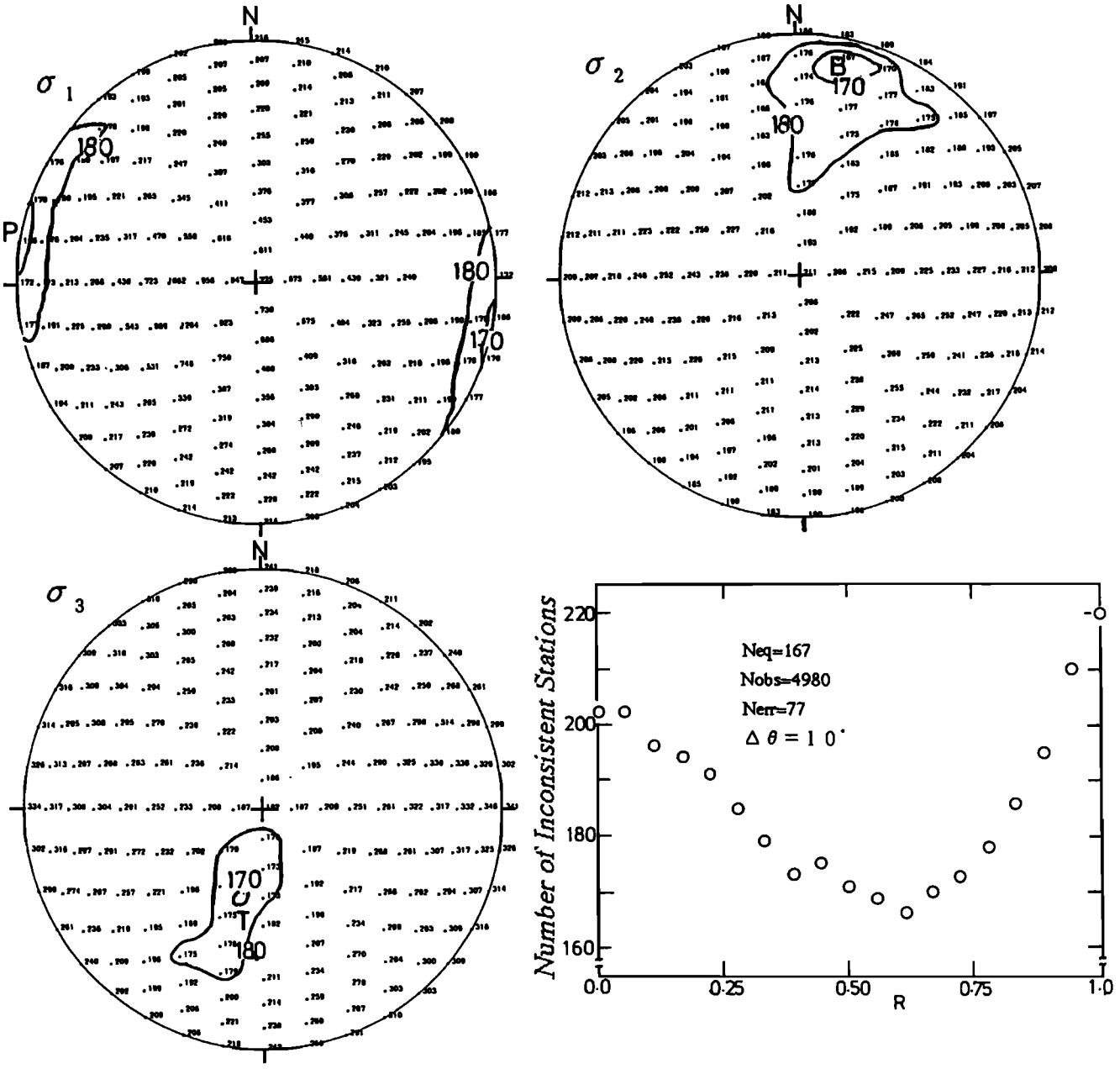

Figure 8. Equal-area projections showing permissible ranges of orientations of the maximum (σ_1), the intermediate (σ_2), and the minimum (σ_3) principal stresses and the distribution of the number of inconsistent stations against R (bottom right). These results are obtained by the use of polarity data from 167 events occurring in the studied area enclosed by the large rectangular in Figure 7. Numerals near contour lines indicate numbers of inconsistent stations. Total number of polarity data used in the analysis is 4980. The total number of inconsistent stations in individual focal mechanism solutions for all events is 77.

present one uses original polarity data of P waves while their method uses parameters of determined focal mechanism solutions.

Gephart and Forsyth [1984] pointed out that it is possible to distinguish fault planes from auxiliary planes by the use of the stress tensor inversion. As shown in Figure 1, if a theoretical slip direction for one of nodal planes is close to an observed slip direction and is not close to the other nodal plane, the fault plane may be easily distinguished from the two planes. However, there is not always a large difference between the two planes. In the case where $\sigma_2 = 0$ and Z_i in (12) is perpendicular to both of P and T in (3) and (7), δ_1 in Figure 1 equals δ_2. In this case, it is impossible to distinguish the fault plane from the auxiliary plane.

There is a large estimation error in the actual determination of focal mechanism solutions. This error is caused mainly by the small number of observation stations and the wrong coverage of stations. In some cases, the estimation error of focal mechanism solutions is larger than the difference between δ_1 and δ_2 in Figure 1. It seems difficult to distinguish fault planes from auxiliary planes without the knowledge of the precise estimation error. The method of *Gephart and Forsyth*

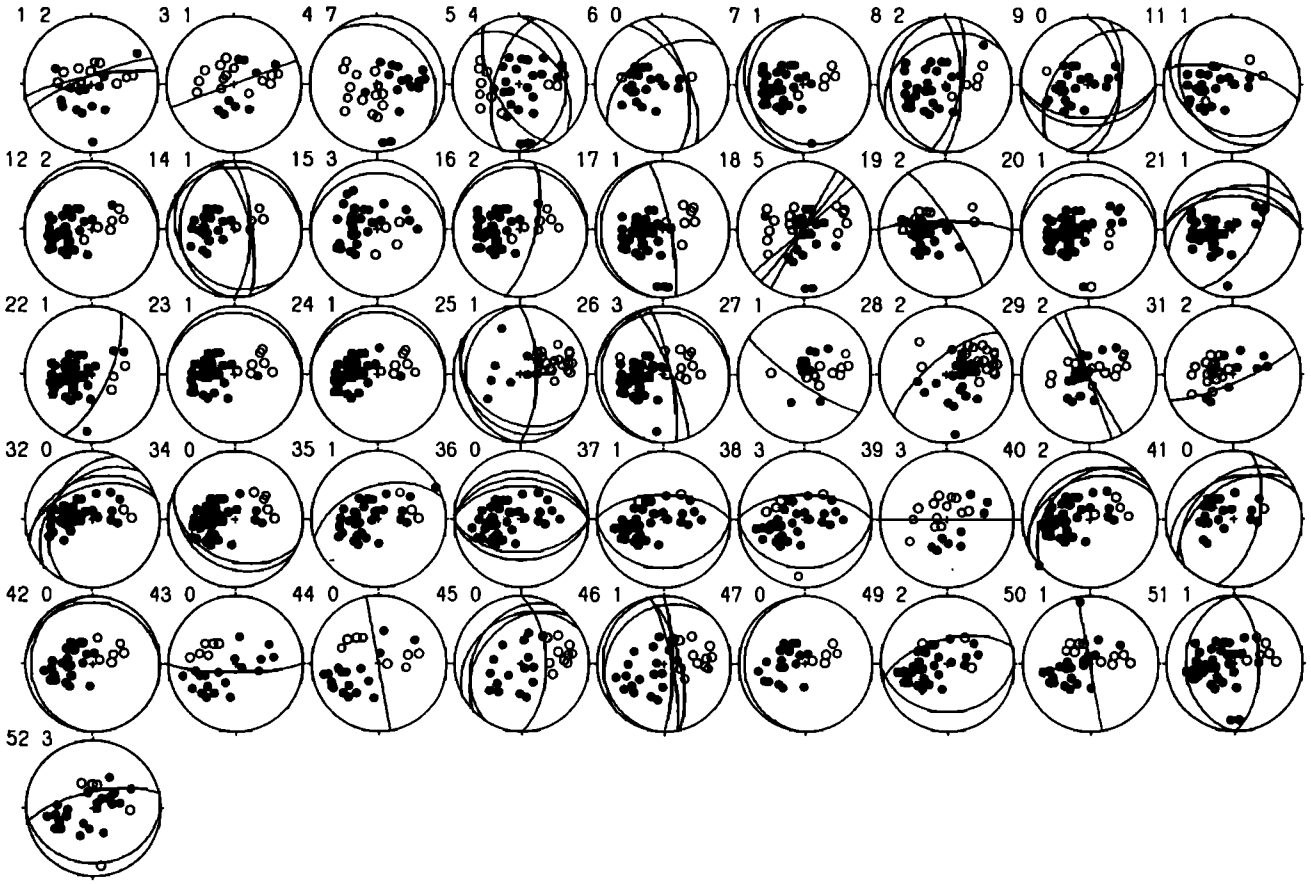

Figure 9. Equal-area projections showing the orientation of fault planes for events occurring in the source region of the main shock shown in the shaded rectangle in Figure 7. Solutions having the minimum number of inconsistent stations are plotted. Two numerals associated with each event are the event identification number and the number of inconsistent polarities. The orientation of fault planes for about 60% of events is distinguished from auxiliary planes.

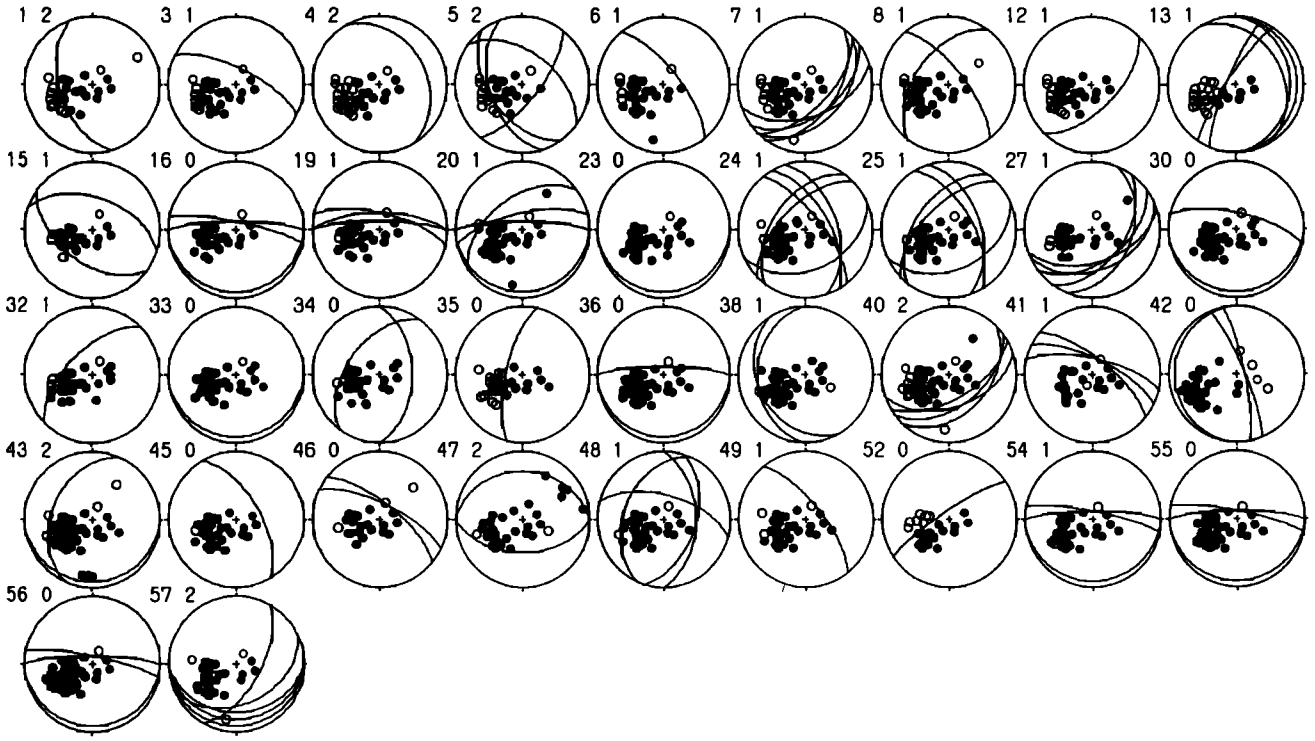

Figure 10. Equal-area projections showing the orientation of fault planes for events occurring in the southwestern part of the aftershock area (small shaded box in Figure 7). Solutions having minimum number of inconsistent stations are plotted. The orientation of fault planes for about 50% of events is distinguished from auxiliary planes.

[1984] was applied by many authors [e.g., *Doser*, 1991; *Gillard et al.*, 1992; *Magee and Zoback*, 1993]. However, these authors did not determine the orientation of fault planes.

The present method inverts polarity data by making a grid search for all combinations of unknown parameters with a certain interval. Therefore we can know a distribution showing the number of inconsistent stations against directions of the fault plane. In a case where a solution for the fault plane of an event is unique, we can distinguish the fault plane from the auxiliary plane. The advantage of the present method is that we can estimate the uniqueness of the solution. A numerical testing is made by applying the present method to an artificial data set from 25 events with 25 × 25 polarity data. It was found that fault planes for about 60% of the events are distinguished from auxiliary planes. There are no events whose auxiliary planes are determined as fault planes. This result suggests that the present method is very effective in distinguishing fault planes from auxiliary planes.

We determined the earthquake-generating stress by applying the present method to porality data from aftershocks of the 1984 western Nagano prefecture earthquake. The obtained direction of the maximum principal stress is horizontal and N80°W-S80°E in the aftershock area. *Ooida et al.* [1989] pointed out that the average direction of pressure axes for focal mechanism solutions of individual aftershocks is nearly horizontal and N63°W. The difference of angles between the two directions is small in the aftershock area.

Zoback et al. [1987] pointed out the existence of a large difference in the orientation of the principal stress obtained from focal mechanisms and from in situ stress measurements along San Andreas fault. Making the stress tensor inversion with the use of focal mechanism solutions for events occurring in the subduction zone of the Tohoku district, Japan, *Magee and Zoback* [1993] showed that the minimum principal stress is almost perpendicular to the subducting plate. The large difference between the two directions suggests that there are many weak planes in a region along San Andreas fault or the subducting plate, which are nearly parallel to the fault or the plate boundary. On the other hand, the 1984 western Nagano prefecture earthquake occurred in an area near an active volcano, where there are no fault traces found on the surface. The consistency of the two directions, the direction of the average pressure axis and that of the obtained maximum principal stress, may suggest that there is no preferred orientations of weakness in the focal region of the 1984 western Nagano prefecture earthquake.

Conclusions

A new method of the stress tensor inversion was developed. Polarity data for many events are inverted to determine stress tensor and the orientation of fault planes. It was shown from the application of the present method to artificial data that this method is effective in distinguishing fault planes from auxiliary planes. The application of this method to actual polarity data from aftershocks of the 1984 western Nagano prefecture earthquake shows that the maximum principal stress in the area is horizontal in the direction of N80°W-S80°E. There are many events having strike-slip faulting, but fault planes of some events are almost perpendicular to the fault plane of the main shock.

Acknowledgments. We have benefited from discussions with T. Hirasawa, Tohoku University, and M. Wyss, University of Alaska. We used the polarity data obtained by the members of the 1986 Joint Seismological Research in western Nagano prefecture and are thankful to them. We also appreciate D. Gillard, University of Alaska, and all the members at the Observation Center for Prediction of Earthquakes and Volcanic Eruptions, Faculty of Science, Tohoku University, for valuable discussions. We are thankful to D.W. Forsyth and an anonymous reviewer who greatly helped us to improve this manuscript.

References

Aoki, H., T. Ooida, I. Fujita, and F. Yamazaki, Seismological study on the 1979 eruption of Ontake Volcano, in *Investigation of Volcanic Activity and Disasters Caused by the 1979 Eruption of Ontake Volcano*(in Japanese), edited by H. Aoki, pp. 55-74, Nagoya University, Nagoya, Japan, 1980.

Castillo, D.A. and W.L. Ellsworth, Seismotectonics of the San Andreas Fault system between Point Arena and Cape Mendocino in north California: Implications for the development and evolution of a young transform, *J. Geophys. Res.*, *98*, 6543-6560, 1993.

Doser, D.I., Faulting within the eastern Baikal rift as characterized by earthquake study, *Tectonophysics, 196*, 109-139, 1991.

Gephart, J.W. and D.W. Forsyth, An improved method for determining the regional stress tensor using earthquake focal mechanism data: Application to the San Fernando Earthquake sequence, *J. Geophys. Res.*, *89*, 9305-9320, 1984.

Gillard, D., M. Wyss, and J.S. Nakata, A seismotectonic model for western Hawaii based on stress tensor inversion from fault plane solutions, *J. Geophys. Res, 97*, 6629-6641, 1992.

Group for the Seismological Research in Western Nagano Prefecture, Data of the 1986 joint seismological research in the western part of Nagano Prefecture, central Japan, *Bull. Earthquake Res. Inst. Univ. Tokyo, 6*, suppl., 1-160, 1989.

Honda, H., A. Masatsuka, and K. Emura, On the mechanism of the earthquakes and the stress producing them in Japan and its vicinity, *Sic Rep. Tohoku Univ.*, Ser. 5, *8*, 186-205, 1956.

Horiuchi, S., K. Emura and T. Hirasawa, Reliability of pressure and tension axes determined by initial motion of *P*-waves from deep earthquakes in and near Japan: The use of J.M.A. network(in Japanese with English abstract), *J. Seismol. Soc. Jpn., Ser.* 2, *25*, 92-104, 1972.

Horiuchi, S., A. Yamamoto, T. Matsuzawa, T. Kono, A. Hasegawa, A. Takagi, A. Ikami, M. Yamada, and H. Aoki, A real-time detection and location of aftershocks of the 1984 Western Nagano Prefecture Earthquake by using personal computer(in Japanese with English abstract), *J. Seismol. Soc. Jpn., Ser.* 2, Ser.2, *33*, 529-539, 1985.

Horiuchi, S., T. Matsuzawa, and A. Hasegawa, Real-time processing system of seismic wave using personal computers, *J. Phys. Earth, 40*, 395-406, 1992a.

Horiuchi, S., and The Members of the 1986 Joint Seismological Research in Western Nagano Prefecture, Hypocenter locations by a dense network, *J. Phys. Earth, 40*, 313-326, 1992b.

Inamori, T., S. Horiuchi, and A. Hasegawa, Location of mid-crustal reflectors by a reflection method using aftershock waveform data in the focal region of the 1984 western Nagano prefecture earthquake, *J. Phys. Earth, 40*, 379-393, 1992.

Isacks, R. and P. Molnar, Distribution of stress in the descending lithosphere from a global survey of focal mechanism solutions of mantle earthquakes, *Rev. Geophys.*, *9*, 103-173, 1971.

Ishida, M., Geometry and relative motion of the Philippine Sea plate and Pacific plate beneath the Kanto-Tokai district, Japan, *J. Geophy. Res.*, *97*, 489-513, 1992.

Jones, L.M., Focal mechanism and the state of stress on the San Andreas fault in southern California, *J. Geophys. Res.*, *93*, 8869-8891, 1988.

Magee, M.E., and M.D. Zoback, Evidence for a weak interplate thrust

fault along the northern Japan subduction zone and implications for the mechanics of thrust faulting and fluid expulsion, *Geology, 21*, 809-812, 1993.

Mizoue, M., and Y. Ishiketa, Detection of melting zone beneath the focal area of the 1984 Western Nagano Prefecture Earthquake and beneath the southeastern foot of Mt. Ontake(in Japanese), *Earth Mon. 10*, 700-705, 1988.

Mount, V.S., and J. Suppe, State of stress near the San Andreas fault: Implications for wrench tectonics, *Geology, 15*, 1143-1146, 1987.

Ooida, T., F. Yamazaki, I. Fujii, and H. Aoki, Aftershock activity of the 1984 Western Nagano Prefecture Earthquake, central Japan, and its relation to earthquake swarms, *J. Phys. Earth, 37*, 401-416, 1989.

Shamir, G., M.D. Zoback, and C.A. Barton, In site stress orientation near the San Andreas fault; Preliminary results to 2.1 km depth from the Cajon Pass scientific drill hole, California, *Geophys. Res. Lett., 15*, 989-992, 1988.

Stauder, W., A compàrison of multiple solutions of focal mechanisms, *Bull. Seismol. Soc. Am., 54*, 927-937, 1964.

Urbancic, T.I., C. Trifu, and P. Young, Microseismicity derived faultplanes and their relationship to focal mechanism, stress inversion, and geological data, *Geophys. Res. Lett., 20*, 2475-2478, 1993.

Wickens, A.J., and J.H. Hodgson, Computer reevaluation of earthquake mechanism solutions, *Publ. Dom. Obs. Ottawa, 33*(1), 1-560, 1967.

Wyss, M., B. Liang, W.R. Tanigawa, and X. Wu, Comparison of orientations of stress and strain tensors based on fault plane solutions in Kaoiki, Hawaii, *J. Geophys. Res., 97*, 4769-4790, 1992.

Yamazaki, F., and The Members of The Joint Seismological Research in Western Nagano Prefecture, Focal mechanism analyses of aftershocks of the 1984 Western Nagano Prefecture Earthquake, *J. Phys. Earth, 40*, 327-341, 1992.

Zoback, M.D., and J.H. Healy, In site stress measurements to 3.5 km depth in the Cajon Pass scientific research borehole; Implications for the mechanics of crustal faulting, *J. Geophys. Res., 97*, 5039-5057, 1992.

Zoback, M.D. et al., New evidence on the state of the San Andreas fault system, *Science, 238*, 1105-1111, 1987.

S. Horiuchi, G. Rocco, and A. Hasegawa, Observation Center for Prediction of Earthquakes and Volcanic Eruptions Faculty of Science, Tohoku University, Sendai 980 Japan. (e-mail: horiuchi@aob.geophys.tohoku.ac.jp, rocco@aob.geophys.tohoku.ac.jp, hasegawa@aob.geophys.tohoku.ac. jp)

(Received April 22, 1994; revised December 9, 1994; accepted December 12, 1994.)